# Supporting Information

**Fluorene-based enamines as low-cost and dopant-free hole transporting materials for high performance and stable perovskite solar cells**

*Sarune Daskeviciute, Cristina Momblona, Kasparas Rakstys, Albertus Adrian Sutanto, Maryte Daskeviciene, Vygintas Jankauskas, Alytis Gruodis, Giedre Bubniene, Vytautas Getautis*, Mohammad Khaja Nazeeruddin**

## EXPERIMENTAL SECTION

Synthetic methods and procedures: Chemicals required for the synthesis were purchased from Sigma-Aldrich and TCI Europe and used as received without additional purification. $^{1}$H NMR spectra were recorded at 400 MHz on a Bruker Avance III spectrometer with a 5 mm double resonance broad band BBO z-gradient room temperature probe, $^{13}$C NMR spectra were collected using the same instrument at 101 MHz. The chemical shifts, expressed in ppm, were relative to tetramethylsilane (TMS). All the NMR experiments were performed at 25 °C. Reactions were monitored by thin-layer chromatography on ALUGRAM SIL G/UV254 plates and developed with UV light. Silica gel (grade 9385, 230–400 mesh, 60 Å, Aldrich) was used for column chromatography. Elemental analysis was performed with an Exeter Analytical CE-440 elemental analyzer, Model 440 C/H/N/. Melting points were measured with Electrothermal MEL-TEMP capillary melting point apparatus.

### *N*$^2$,*N*$^2$,*N*$^7$,*N*$^7$-tetrakis[2,2-bis(4-methoxyphenyl)vinyl]-9*H*-fluorene-2,7-diamine (V1275)

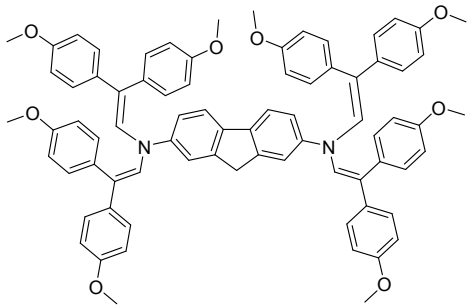

2,7-diaminofluorene (0.3 g, 1.5 mmol) was dissolved in tetrahydrofuran (9 mL + volume of the Dean-Stark trap), (+/-)camphor-10-sulphonic acid (0.36 g, 1.5 mmol) was added and the mixture was heated at reflux for 20 minutes. Afterwards, 2,2-bis(4-methoxyphenyl)acetaldehyde (2.4 g, 9.2 mmol) was added and reflux was continued using a Dean-Stark trap for 6 hours. After cooling to room temperature, reaction mixture was extracted with ethyl acetate. The organic layer was dried over anhydrous $Na_2SO_4$, filtered and solvent evaporated. The

crude product was crystallized from ethanol (30 mL). The obtained crystals were filtered off and washed with hot ethanol for three times. The product was recrystallized from acetone/ethanol 1:1 gave as light yellow-green crystals (1.14 g, 60%). $^{1}$H NMR (400 MHz, $CDCl_3$) δ 7.60 (d, *J* = 8.4 Hz, 2H), 7.34 – 7.20 (m, 2H), 7.19 – 6.94 (m, 10H), 6.84 (d, *J* = 8.4 Hz, 8H), 6.67 (d, *J* = 8.4 Hz, 8H), 6.49 (d, *J* = 8.4 Hz, 8H), 5.82 (s, 4H), 4.04 – 3.57 (m, 26H). $^{13}$C NMR (101 Mhz, $CDCl_3$) δ 159.01, 158.71, 144.37, 132.82, 130.66, 130.18, 128.85, 114.43, 113.92, 113.63, 113.05, 55.46, 55.26, 37.05 ppm. Anal. calcd for $C_{77}H_{68}N_2O_8$: C, 80.46; H, 5.96; N, 2.44; found: C, 80.14; H, 5.82; N, 2.48.

**9,9-dibenzyl-*N*$^2$,*N*$^2$,*N*$^7$,*N*$^7$-tetrakis[2,2-bis(4-methoxyphenyl)vinyl]-9*H*-fluorene-2,7-diamine (V1227)**

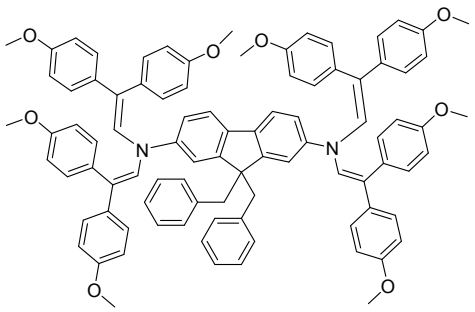

Compound **V1275** (0.5 g, 0.4 mmol) in dimethylsulfoxyde (20 mL) was dissolved and purged with argon for 30 minutes. Afterwards, benzyltriethylammonium chloride (0.01 g, 0.04 mmol) and 50% NaOH (0.15 mL) solution were added. The color of the reaction turned black and then benzyl bromide (0.16 g, 1.0 mmol) was slowly added dropwise under argon atmosphere and stirred at room temperature for 96 hours. The reaction mixture was filtered off and washed with water three times. The crude product was purified by column chromatography using 1:4 v/v tetrahydrofuran/*n*-hexane as an eluent to collect **V1227** as a pale brown solid (0.29 g, 50%). $^{1}$H NMR (400 MHz, acetone-$d_6$) δ 7.56 (d, *J* = 8.0 Hz, 2H), 7.31 – 6.78 (m, 30H), 6.71 (d, *J* = 8.4 Hz, 8H), 6.50 (d, *J* = 8.4 Hz, 8H), 5.97 – 5.66 (m, 4H), 3.85 (d, *J* = 48.8 Hz, 24H), 3.53 – 3.14 (m, 4H). $^{13}$C NMR (101 MHz, acetone) δ 159.35, 159.03, 148.60, 136.29, 134.30, 132.53, 130.68, 130.54, 128.84, 127.22, 127.14, 126.52, 113.86, 113.50, 112.98, 60.05, 54.88, 54.61, 10.95 ppm. Anal. calcd for $C_{91}H_{80}N_2O_8$: C, 82.20; H, 6.06; N, 2.11; found: C, 82.54; H, 6.11; N, 2.15.

***N*²,*N*²,*N*⁷,*N*⁷-tetrakis[2,2-bis(4-methoxyphenyl)vinyl]-9,9-dipropyl-9*H*-fluorene-2,7-diamine (V1235)**

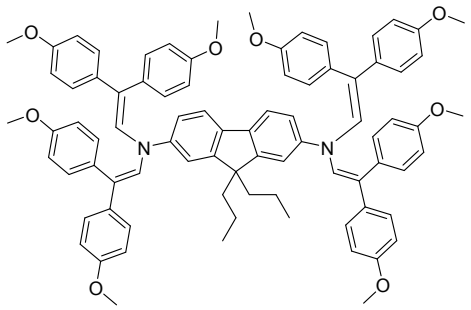

Compound **V1275** (0.5 g, 0.4 mmol) in dimethylsulfoxyde (20 mL) was dissolved and purged with argon for 30 minutes. Afterwards, benzyltriethylammonium chloride (0.01 g, 0.04 mmol) and 50% NaOH (0.15 mL) solution were added. The color of the reaction turned black and then bromopropane (0.12 g, 1.0 mmol) was slowly added dropwise under argon atmosphere and stirred at room temperature for 72 hours. The reaction mixture was filtered off and washed with water three times. The crude product was purified by column chromatography using 1:4 v/v tetrahydrofuran/*n*-hexane as an eluent to collect **V1235** as a yellow solid (0.28 g, 52%). $^{1}$H NMR (400 MHz, $CDCl_3$) δ 7.48 (d, *J* = 8.0 Hz, 2H), 7.12 – 6.94 (m, 12H), 6.85 (d, *J* = 8.8 Hz, 8H), 6.66 (d, *J* = 8.8 Hz, 8H), 6.51 (d, *J* = 8.8 Hz, 8H), 5.81 (s, 4H), 3.81 (d, *J* = 37.2 Hz, 24H), 1.99 – 1.81 (m, 4H), 0.88 – 0.60 (m, 10H). $^{13}$C NMR (101 MHz, $CDCl_3$) δ 158.79, 158.54, 149.08, 134.23, 132.65, 130.45, 128.79, 119.03, 113.71, 112.84, 111.90, 59.52, 55.25, 55.07, 17.74, 14.12, 11.52 ppm. Anal. calcd for $C_{83}H_{80}N_2O_8$: C, 80.82; H, 6.54; N, 2.27; found: C, 80.64; H, 6.61; N, 2.30.

***N*²,*N*²,*N*⁷,*N*⁷-tetrakis[2,2-bis(4-methoxyphenyl)vinyl]-9,9-dihexyl-9*H*-fluorene-2,7-diamine (V1236)**

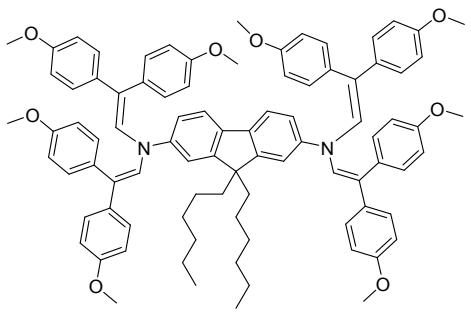

Compound **V1275** (0.5 g, 0.4 mmol) in dimethylsulfoxyde (20 mL) was dissolved and purged with argon for 30 minutes. Afterwards, benzyltriethylammonium chloride (0.01 g, 0.04 mmol) and 50% NaOH (0.15 mL) solution were added. The color of the reaction turned black and then bromohexane (0.16 g, 1.0 mmol) was slowly added dropwise under argon atmosphere and stirred at room temperature for 26 hours. The reaction mixture was filtered off and washed repeatedly with water three times. The crude product was purified by column chromatography

using 4:21 v/v tetrahydrofuran/*n*-hexane as an eluent to collect **V1236** as a yellow solid (0.36 g, 63%). $^{1}$H NMR (400 MHz, $CDCl_3$) δ 7.52 (d, *J* = 8.0 Hz, 2H), 7.12 – 6.93 (m, 12H), 6.85 (d, *J* = 8.4 Hz, 8H), 6.65 (d, *J* = 8.4 Hz, 8H), 6.50 (d, *J* = 8.8 Hz, 8H), 5.81 (s, 4H), 3.81 (d, *J* = 38.0 Hz, 24H), 1.97 – 1.82 (m, 4H), 1.21 – 1.01 (m, 12H), 0.85 – 0.66 (m, 10H) ppm. $^{13}$C NMR (101 MHz, $CDCl_3$) δ 158.99, 158.69, 152.04, 134.48, 132.95, 130.64, 128.90, 119.25, 115.91, 113.92, 113.02, 111.31, 55.38, 55.26, 40.11, 31.39, 29.38, 23.62, 22.48, 14.12 ppm. Anal. calcd for $C_{89}H_{92}N_2O_8$: C, 81.12; H, 7.04; N, 2.13; found: C, 81.24; H, 7.11; N, 2.10.

**$N^2$,$N^2$,$N^7$,$N^7$-tetrakis[2,2-bis(4-methoxyphenyl)vinyl]-9,9-dimethyl-9*H*-fluorene-2,7-diamine (V1237)**

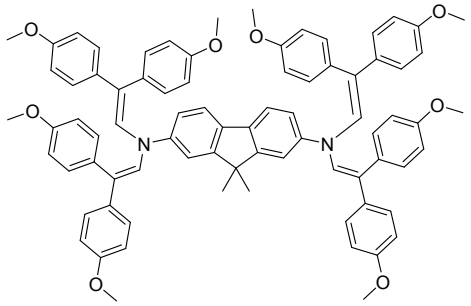

Compound **V1275** (0.5 g, 0.4 mmol) in dimethylsulfoxyde (20 mL) was dissolved and purged with argon for 30 minutes. Afterwards, benzyltriethylammonium chloride (0.01 g, 0.04 mmol) and 50% NaOH (0.15 mL) solution were added. The color of the reaction turned black and then iodomethane (0.14 g, 1.0 mmol) was slowly added dropwise under argon atmosphere and stirred at room temperature for 120 hours. The reaction mixture was filtered off and washed with water three times. The crude product was purified by column chromatography using 1:4 v/v tetrahydrofuran/*n*-hexane as an eluent to collect **V1237** as a yellow solid (0.26 g, 51%). $^{1}$H NMR (400 MHz, $CDCl_3$) δ 7.54 (d, *J* = 8.0 Hz, 2H), 7.19 – 6.94 (m, 12H), 6.87 (d, *J* = 8.4 Hz, 8H), 6.66 (d, *J* = 8.4 Hz, 8H), 6.53 (d, *J* = 8.4 Hz, 8H), 5.96 – 5.70 (m, 4H), 3.84 (d, *J* = 36.8, 24H), 1.46 (s, 6H). $^{13}$C NMR (101 MHz, $CDCl_3$) δ 158.98, 158.68, 155.02, 132.82, 132.23, 130.65, 128.90, 116.10, 113.90, 113.01, 111.03, 55.43, 55.24, 47.14, 27.56 ppm. Anal. calcd for $C_{79}H_{72}N_2O_8$: C, 80.59; H, 6.16; N, 2.38; found: C, 80.74; H, 6.11; N, 2.35.

**Device fabrication:**

Fluorine-doped tin oxide (FTO) coated glass was laser scribed to avoid direct contact between electrodes. The substrates were cleaned in a 2% Helmanex solution, deionized water and ethanol in an ultrasonic bath for 10 minutes each, followed by a 15 min of UV/$O_3$ treatment. A thin film of compact $TiO_2$ (30 nm) was deposited by spray pyrolysis from a titanium diisopropoxide bis(acetylacetonate)(TAA) (Sigma Aldrich) in isopropanol solution (1:15 v/v) at 450ºC. The layers were kept at 450ºC during 30 minutes. The mesoporous $TiO_2$ layers were prepared by spin-coating a diluted $TiO_2$ paste (Dyesol 30 NR-D) solution (1 gr. in 9 mL ethanol) at 5000 rpm (1000 rpm/s, 15 s) and sintered on a hot plate at 500 ºC for 30 min. Thereafter, a $SnO_2$ layer (20 nm) was prepared by spin-coating $SnCl_4$ (Acros) dissolved in deionized water (12 µl in 988 µl water) at 3000 rpm for 30 s (acc. 1000 rpm/s), followed by annealing at 190 ºC for 1 h. The $[(FAPbI_3)_{0.87}(MAPbBr_3)_{0.13}]_{0.92}(CsPbI_3)_{0.08}$ perovskite solution was prepared by dissolving 17.41 mg MABr, 27.02 mg CsI, 57.06 mg $PbBr_2$, 178.94 mg FAI and 548.60 mg $PbI_2$ in 1 ml of DMF:DMSO (0.78:0.22 v/v). The perovskite solution was then spin coated at 2000 rpm for 10 s, followed by 5000 rpm for 30 s. During spinning in the second step, 110 µl of chlorobenzene was dropped on the sample at the 15 s before finishing the process. The films were annealed at 100ºC for 1 h inside the glove box. Once the samples were cooled down, spiro-OMeTAD or V-series HTMs were deposited on top of the perovskite layer by spin-coating. The spiro-OMeTAD was deposited from a 60 mM solution in chlorobenzene with *tert*-butylpyridine (tBP), tris(2-(1*H*-pyrazol-1-yl)-4-*tert*-butylpyridine)cobalt(III) (FK209) and tris(bis(trifluoromethylsulfonyl)imide) (LiTFSI) as additives. The concentration of doped- and dopant-free V-series HTMs were 20 and 15 mM, respectively. The molar ratio of additives for spiro-OMeTAD and each doped HTM solution was 0.5 for LiTFSI from a 1.8 M stock solution in acetonitrile, 3.3 for tBP and 0.03 for FK209 from a 0.25 M stock solution in acetonitrile. Finally, 70 nm of Au was thermally evaporated as top electrode.

The *J – V* characteristics were measured by using a 2400 Keithley system in a scan rate of 50 mV $s^{-1}$ and 10 mV voltage step in combination with a Xe–lamp Oriel sol3A sun simulator (Newport Corporation), previously calibrated to AM1.5G standard conditions by using the reference cell Oriel 91150 V. The devices were measured with 2s light soaking and with an illumination area through a shadow mask of 16 $mm^2$. Prior to evaluate the long-term stability of the devices, *J-V* curves mere measured in a Xe-lamp solar simulator in ambient atmosphere. The devices were measured with 2s light soaking and with an illumination area of 16 $mm^2$ limited by a shadow mask and without cooling system. After the measurement of the *J-V* characteristics, the devices were placed for stability test. The stability test was performed as maximum power tracking under 100 mW $cm^{-2}$ illumination with a LED power source. Note that during the stability test the samples were placed in a measurement box purged continuously with nitrogen gas at 0% humidity in order to create an inert atmosphere. The box temperature was kept at 25 °C by a cooling system. A shadow mask of 16 $mm^2$ was used to define the illumination area during the

long-term stability test. EQE was measured with IQE200B Quantum Efficiency Measurement System (Oriel, Newport). Scanning electron microscopy (SEM) images were recorded by in-lens detector of FEI Teneo Schottky Field Emission SEM at tension of 5 kV. The steady-state photoluminescence spectra of the perovskite and perovskite/HTM thin films were measured and recorded using Fluorolog3-22 spectrofluorometer. The spectra were recorded upon excitation at 625 nm with the sample illuminated from front side (perovskite or HTM side).

| Chemical | Weight reagent (g/g) | Weight solvent (g/g) | Weight workup (g/g) | Price of chemical (€/kg) | Cost of chemical (€/g product) | Total cost (€/g) |
|---|---|---|---|---|---|---|
| 4-Bromoanisole | 3.98 | | | 25.2 | 0.10 | |
| Formic acid | 20 | | | 3.87 | 0.08 | |
| Sulfuric acid | 4 | | | 2.63 | 0.01 | |
| Methyl methoxyacetate | 0.739 | | | 304 | 0.22 | |
| Magnesium | 0.518 | | | 104 | 0.05 | |
| Diethyl ether | | 200 | | 6.92 | 1.38 | |
| Ethyl acetate | | | 150 | 2.85 | 0.43 | |
| **2,2-bis(4-methoxyphenyl)acetaldehyde** | 29.237 | 200 | 150 | | | 2.28 |
| 2,2-bis(4-methoxyphenyl)acetaldehyde | 1.426 | | | 2300 | 3.28 | |
| 2,7-Diaminofluorene | 0.182 | | | 31480 | 5.73 | |
| 10-Camphorsulfonic acid | 0.218 | | | 260 | 0.06 | |
| Toluene | | 9 | | 2.46 | 0.02 | |
| Ethyl acetate | | | 200 | 2.85 | 0.57 | |
| $Na_2SO_4$ | | | 50 | 6.08 | 0.30 | |
| Ethanol | | | 80 | 6.08 | 0.49 | |
| ***N*²,*N*²,*N*⁷,*N*⁷-tetrakis(2,2-bis(4-methoxyphenyl)vinyl)-9*H*-fluorene-2,7-diamine (V1275)** | 1.826 | 9 | 330 | | | 10.45 |
| *N*²,*N*²,*N*⁷,*N*⁷-tetrakis(2,2-bis(4-methoxyphenyl)vinyl)-9*H*-fluorene-2,7-diamine | 1.78 | | | 10450 | 18.60 | |
| Benzyltriethylammonium chloride | 0.024 | | | 159.8 | 0.00 | |
| 1-Bromopropane | 0.428 | | | 64 | 0.03 | |
| Sodium hydroxide | 0.274 | | | 38.08 | 0.01 | |
| Dimethyl sulfoxide | | 53 | | 47.27 | 2.51 | |
| Ethyl acetate | | | 200 | 2.85 | 0.57 | |
| $Na_2SO_4$ | | | 50 | 6.08 | 0.30 | |
| THF | | | 10 | 8.88 | 0.09 | |
| Ethanol | | | 10 | 6.08 | 0.06 | |
| ***N*²,*N*²,*N*⁷,*N*⁷-tetrakis[2,2-bis(4-methoxyphenyl)vinyl]-9,9-dipropyl-9*H*-fluorene-2,7-diamine (V1235)** | 2.506 | 53 | 270 | | | 22.17 |

**Table S1**. Materials, quantities and cost for the synthesis of **V1275** and **V1235**.

**V1275a**

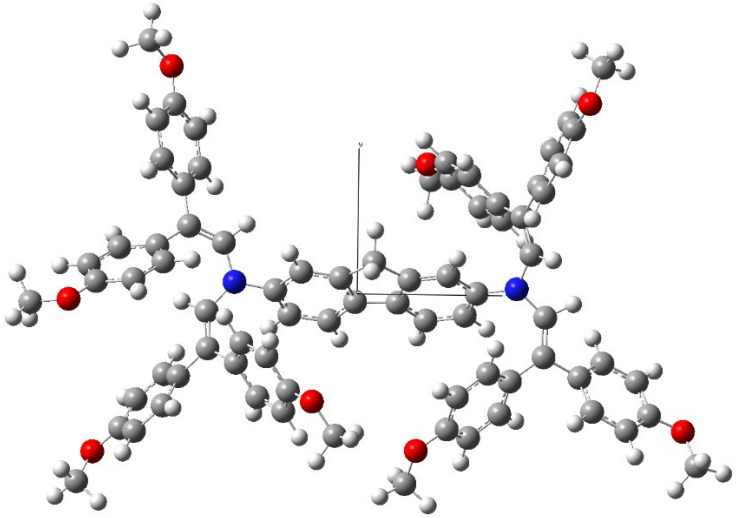

**V1275b**

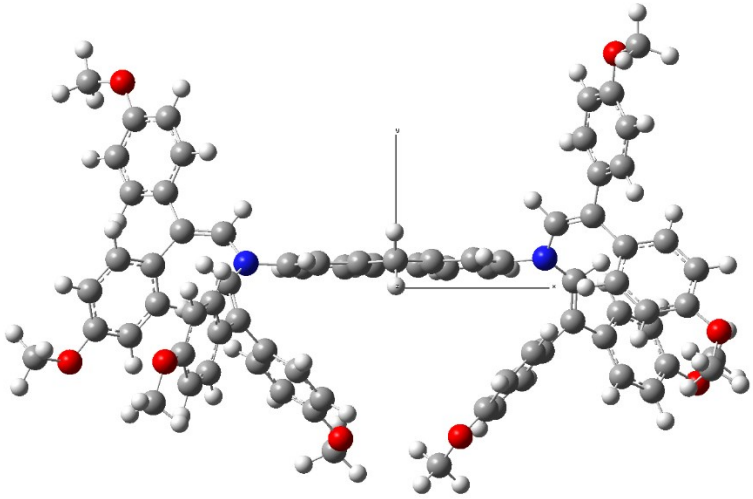

**Figure S1**. Optimized molecular structures of **V1275** in XY projections. Gaussian09, B3LYP/6-31G.

**V1237a**

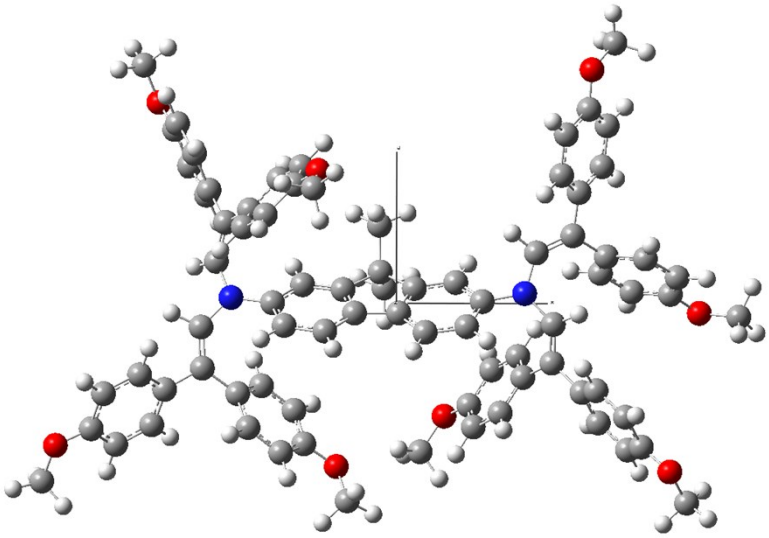

**V1237b**

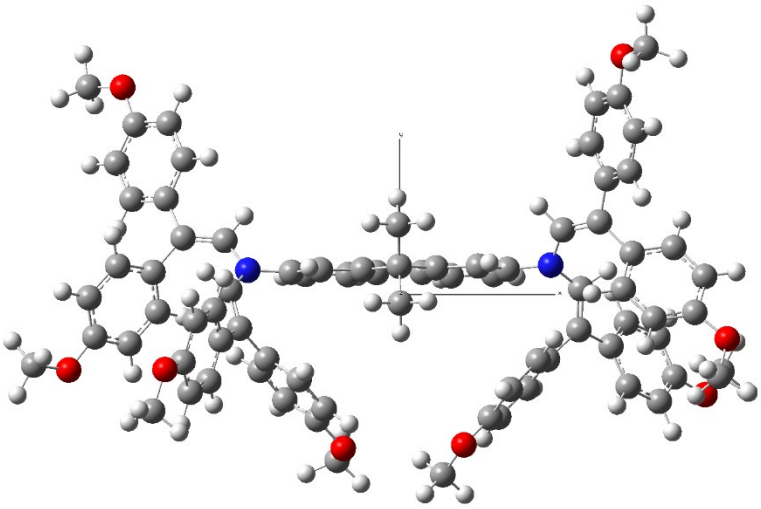

**Figure S2**. Optimized molecular structures of **V1237** in XY projections. Gaussian09, B3LYP/6-31G.

**V1227a**

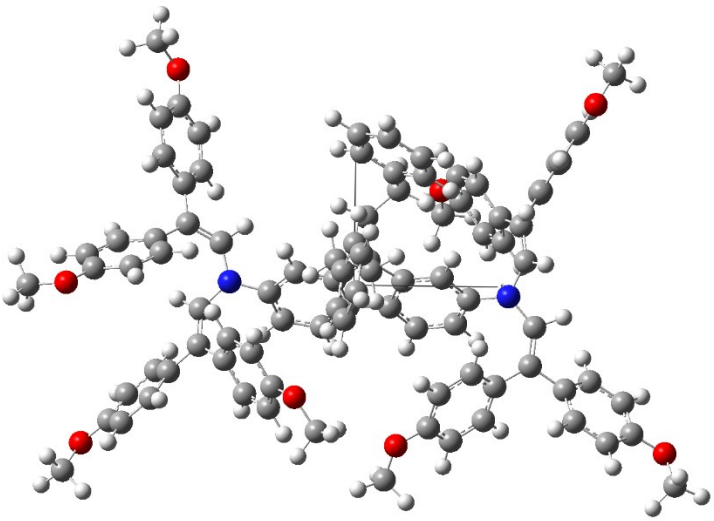

**V1227b**

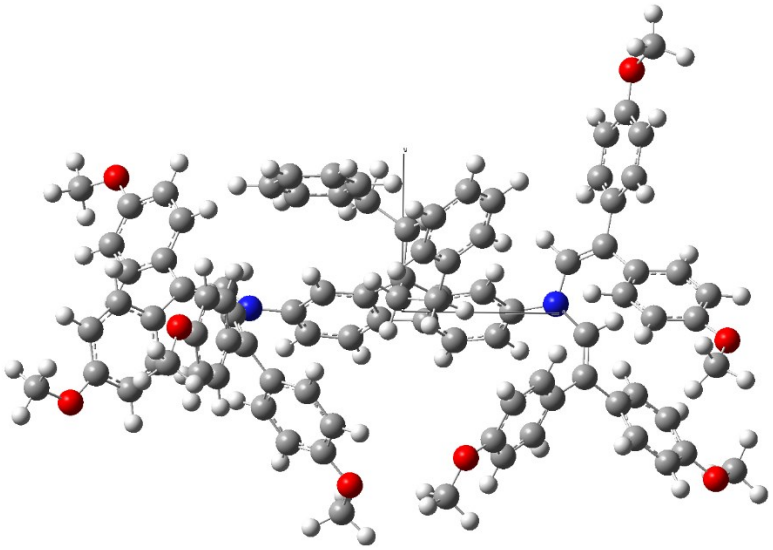

**Figure S3**. Optimized molecular structures of **V1227** in XY projections. Gaussian09, B3LYP/6-31G.

**Table S2.** Parameters of electronic absorption spectra of **V1227**, **V1237**, **V1275**, simulated by *Gaussian09*, semiempirical TD routine (for singlets only). Population of three lowest excited states: $S_1$, $S_2$, $S_3$. Transition energy $\Delta E$ and corresponding oscillator

| strength *f*. | | | | | | |
|---|---|---|---|---|---|---|
| Transition | $S_0 \rightarrow S_1$ | | $S_0 \rightarrow S_2$ | | $S_0 \rightarrow S_3$ | |
| Parameters | *ΔE*, eV | *f* | *ΔE*, eV | *f* | *ΔE*, eV | *f* |
| **V1227a** | 2.89 | 0.57 | 2.98 | 0.46 | 3.19 | 0.07 |
| **V1227b** | 2.90 | 0.71 | 3.15 | 0.10 | 3.21 | 0.44 |
| **V1237a** | 2.91 | 0.59 | 2.97 | 0.42 | 3.19 | 0.12 |
| **V1237b** | 2.90 | 0.75 | 3.15 | 0.17 | 3.21 | 0.53 |
| **V1275a** | 2.93 | 0.57 | 2.98 | 0.47 | 3.20 | 0.21 |
| **V1275b** | 2.92 | 0.77 | 3.17 | 0.23 | 3.21 | 0.54 |

**Table S3.** Parameters of electronic absorption spectra of **V1227**, **V1237**, **V1275**, simulated by *Gaussian09*, semiempirical TD routine (for singlets only). Population of "spectroscopic" states (from ground states to excited states) ΔT and corresponding set of MO with contribution coefficient *k* (contribution of the respective excitation to the configurational interaction wavefunction).

| | a conformer | | | b conformer | | |
|---|---|---|---|---|---|---|
| | ΔT | Transition between MO | *k* | ΔT | Transition between MO | *k* |
| **V1227** | $S_0 \rightarrow S_1$ | HOMO→LUMO | 0.53 | $S_0 \rightarrow S_1$ | HOMO→LUMO | 0.69 |
| | $S_0 \rightarrow S_2$ | HOMO→LUMO+1 | 0.55 | $S_0 \rightarrow S_2$ | HOMO-1→LUMO | 0.66 |
| | $S_0 \rightarrow S_3$ | HOMO-1→LUMO+1 | 0.55 | $S_0 \rightarrow S_3$ | HOMO→LUMO+1 | 0.58 |
| **V1237** | $S_0 \rightarrow S_1$ | HOMO→LUMO | -0.44 | $S_0 \rightarrow S_1$ | HOMO→LUMO | 0.69 |
| | | HOMO→LUMO+1 | 0.52 | | | |
| | $S_0 \rightarrow S_2$ | HOMO→LUMO | 0.48 | $S_0 \rightarrow S_2$ | HOMO-1→LUMO | 0.61 |
| | | HOMO→LUMO+1 | 0.45 | | | |
| | $S_0 \rightarrow S_3$ | HOMO-1→LUMO | -0,39 | $S_0 \rightarrow S_3$ | HOMO→LUMO+1 | 0.42 |
| | | HOMO→LUMO+2 | 0.46 | | HOMO→LUMO+2 | 0.47 |
| **V1275** | $S_0 \rightarrow S_1$ | HOMO→LUMO | 0.47 | $S_0 \rightarrow S_1$ | HOMO→LUMO | 0.69 |
| | | HOMO→LUMO+1 | 0.49 | | | |
| | $S_0 \rightarrow S_2$ | HOMO→LUMO | -0.45 | $S_0 \rightarrow S_2$ | HOMO-1→LUMO | 0.56 |
| | | HOMO→LUMO+1 | 0.49 | | HOMO→LUMO+1 | 0.31 |
| | $S_0 \rightarrow S_3$ | HOMO→LUMO+2 | 0.55 | $S_0 \rightarrow S_3$ | HOMO→LUMO+1 | 0.40 |
| | | | | | HOMO→LUMO+2 | 0.49 |

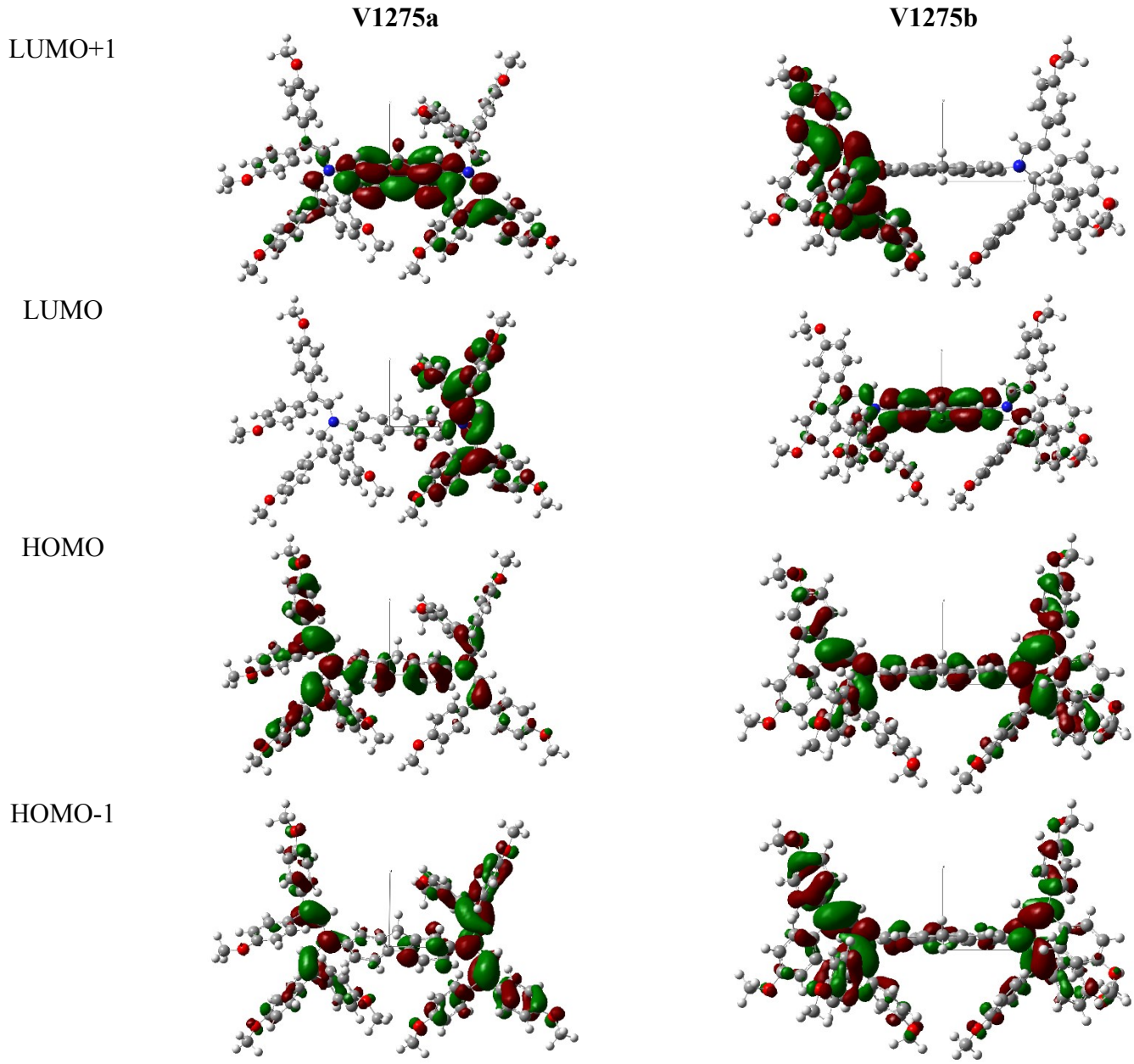


**Figure S4**. **V1275** structure, a and b conformers, XY projection. Distributions of electron density for the HOMO-1, HOMO, LUMO and LUMO+1.

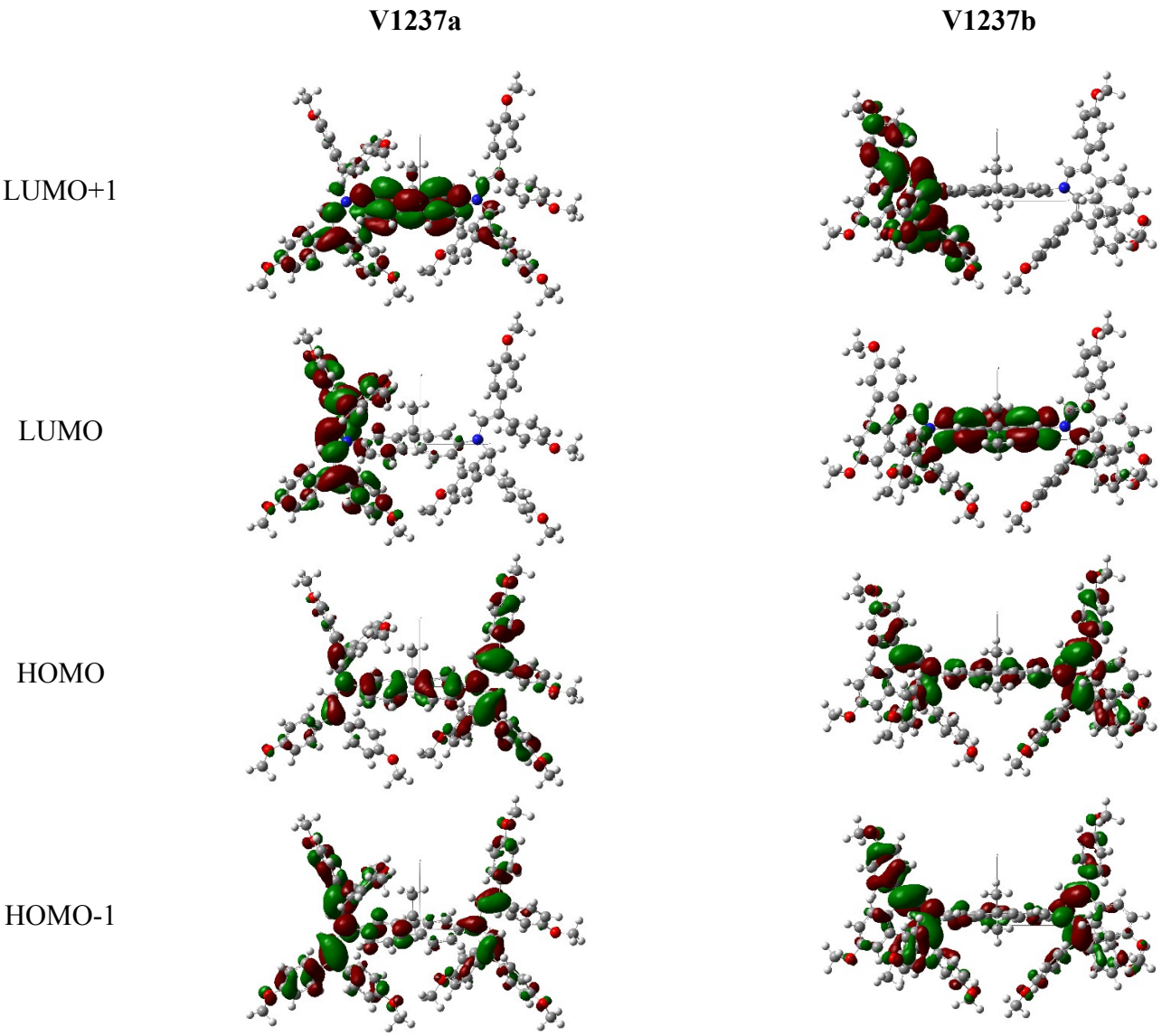


**Figure S5**. **V1237** structure, a and b conformers, XY projection. Distributions of electron density for the HOMO-1, HOMO, LUMO and LUMO+1.

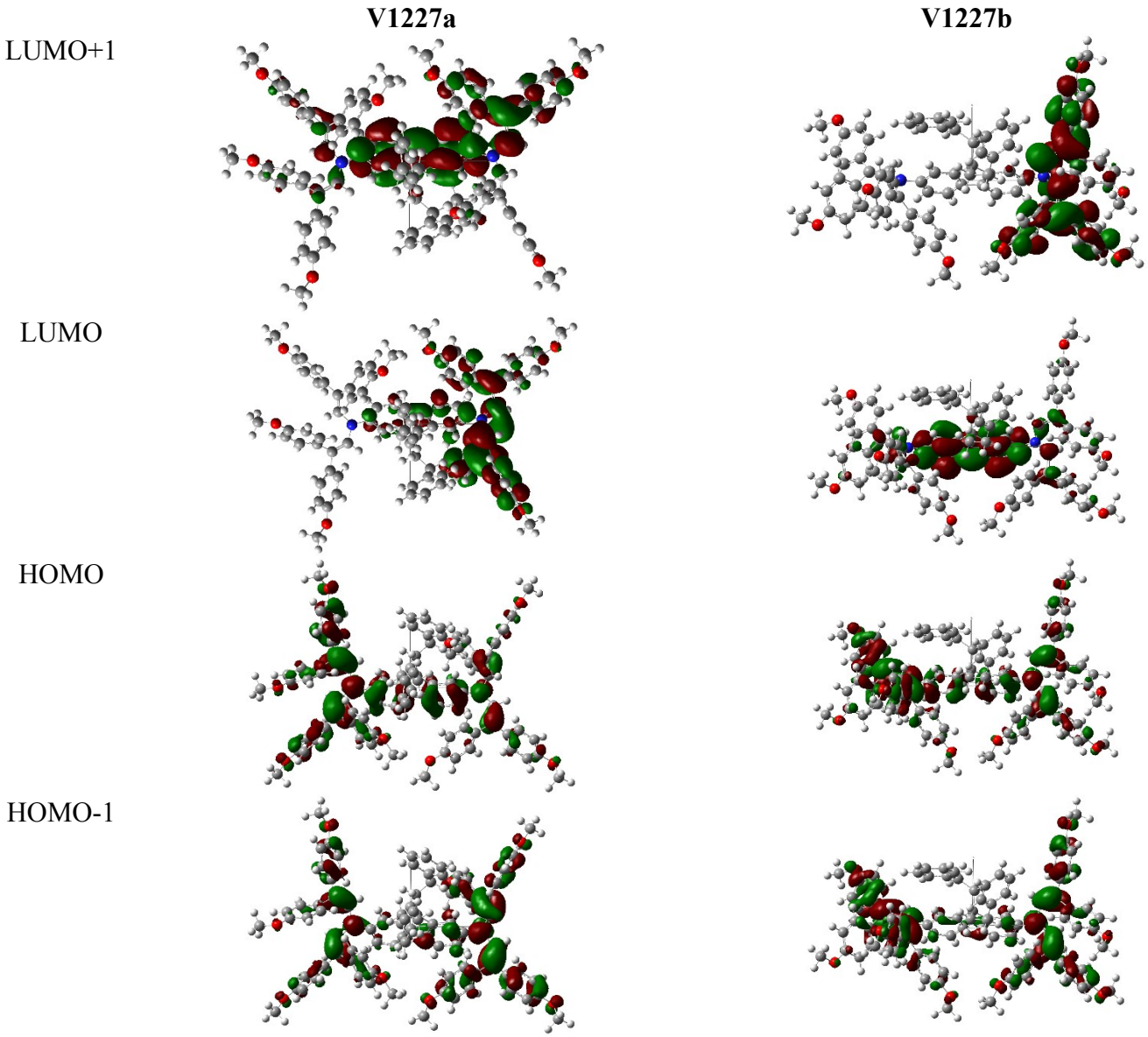


**Figure S6**. **V1227** structure, a and b conformers, XY projection. Distributions of electron density for the HOMO-1, HOMO, LUMO and LUMO+1.

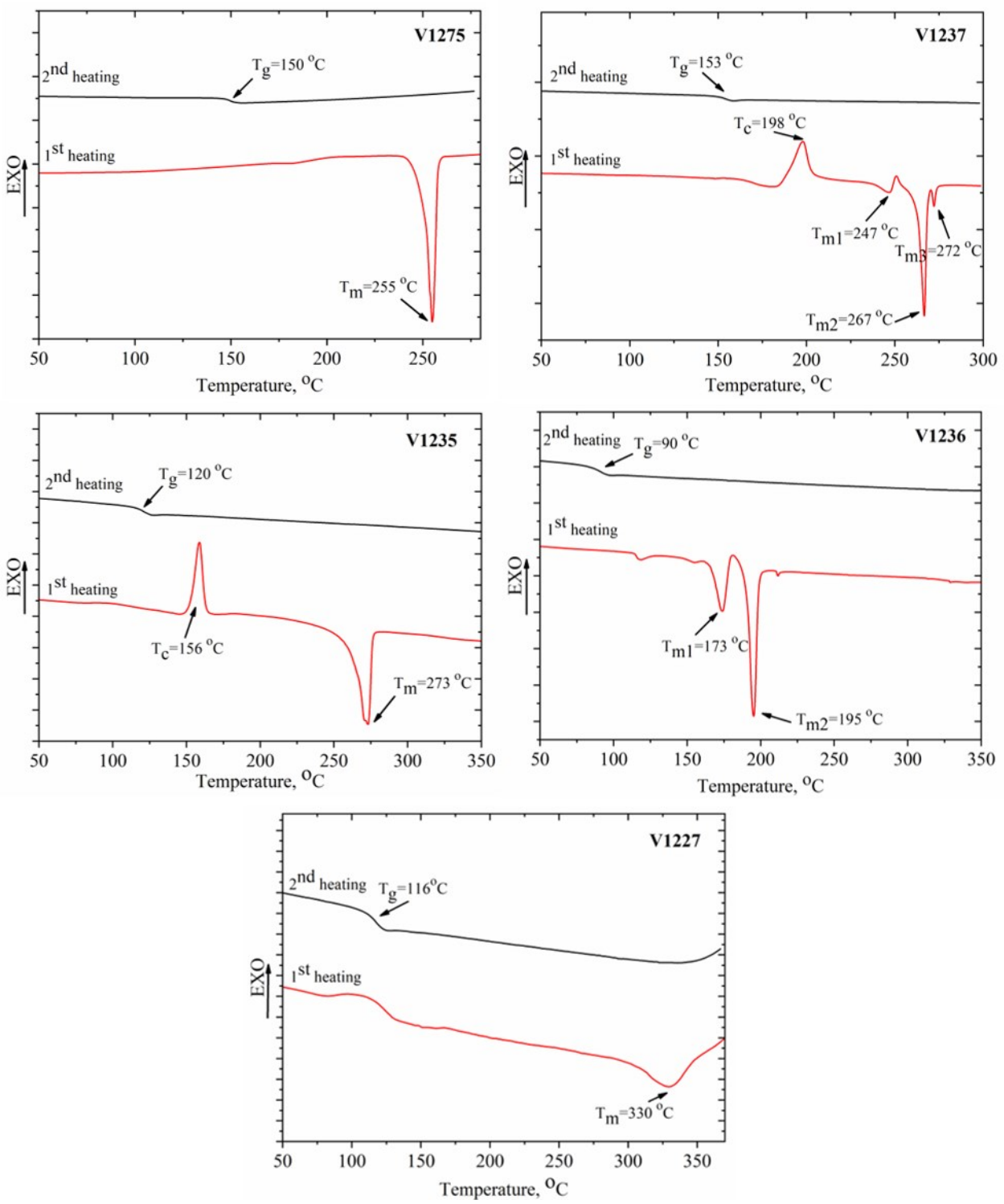


**Figure S7**. DSC first and second heating curves of HTMs (scan rate 10 ºC/min, $N_2$ atmosphere).

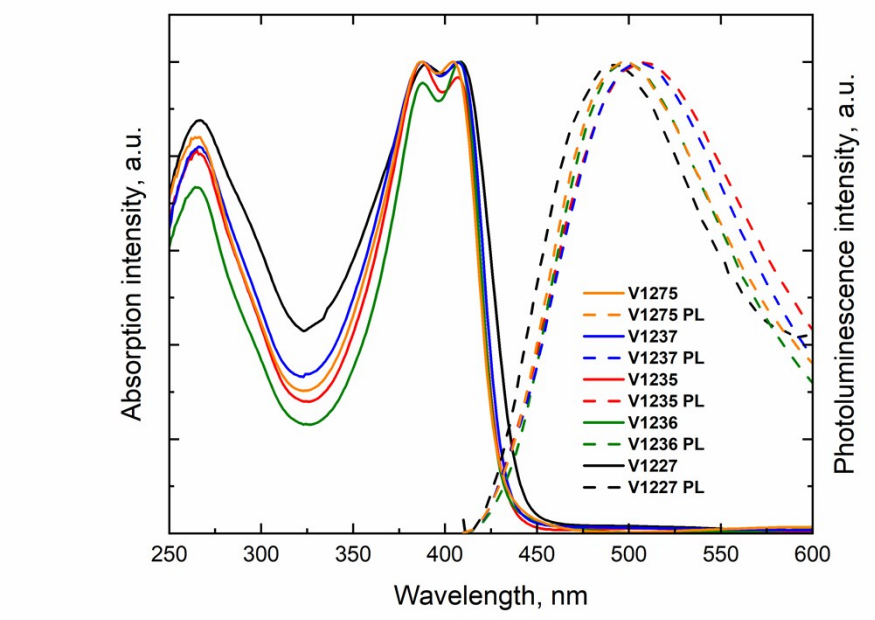


**Figure S8**. UV−Vis absorption (solid line) and photoluminescence (dashed line) spectra of V-series HTMs thin films.

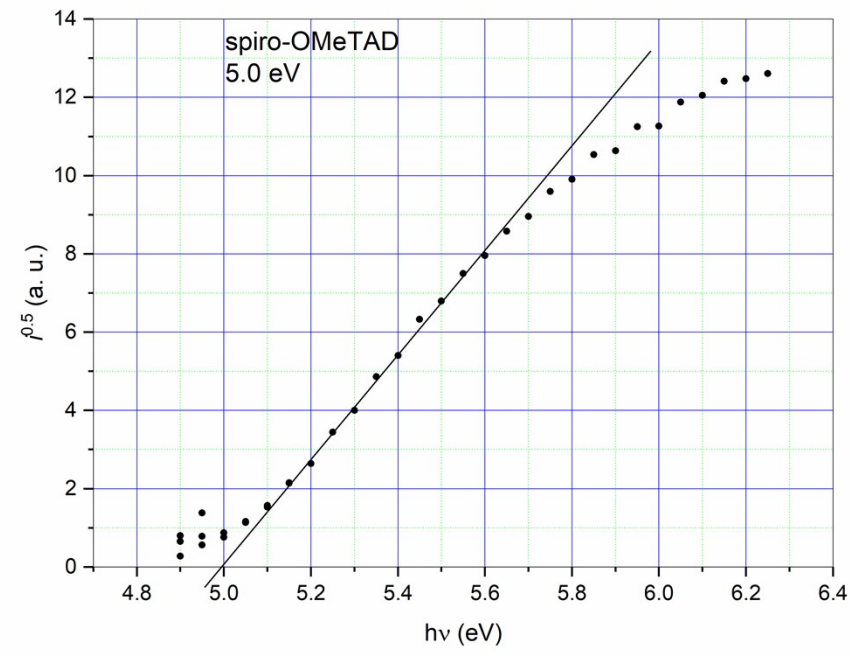


**Figure S9**. Photoemission in air spectra of the spiro-OMeTAD.

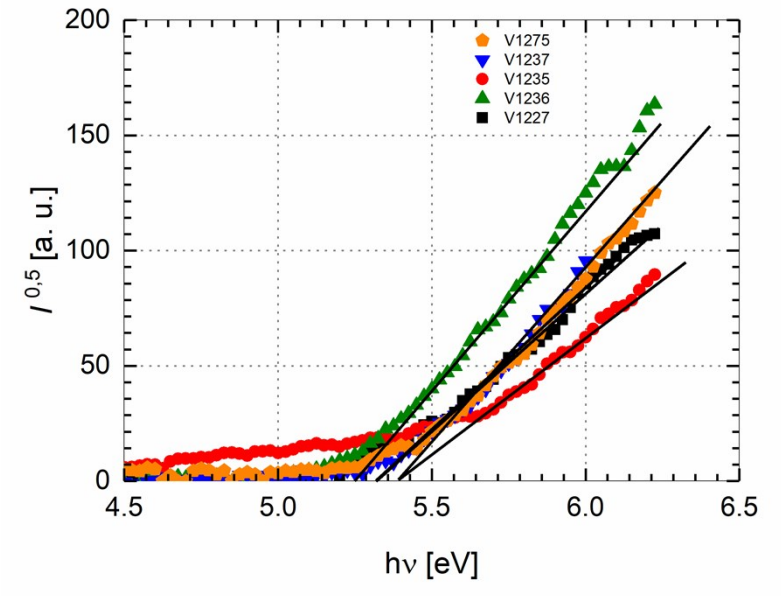


**Figure S10**. Photoemission in air spectra of the doped charge transporting layers **V1275**, **V1237**, **V1235**, **V1236**, and **V1227**.

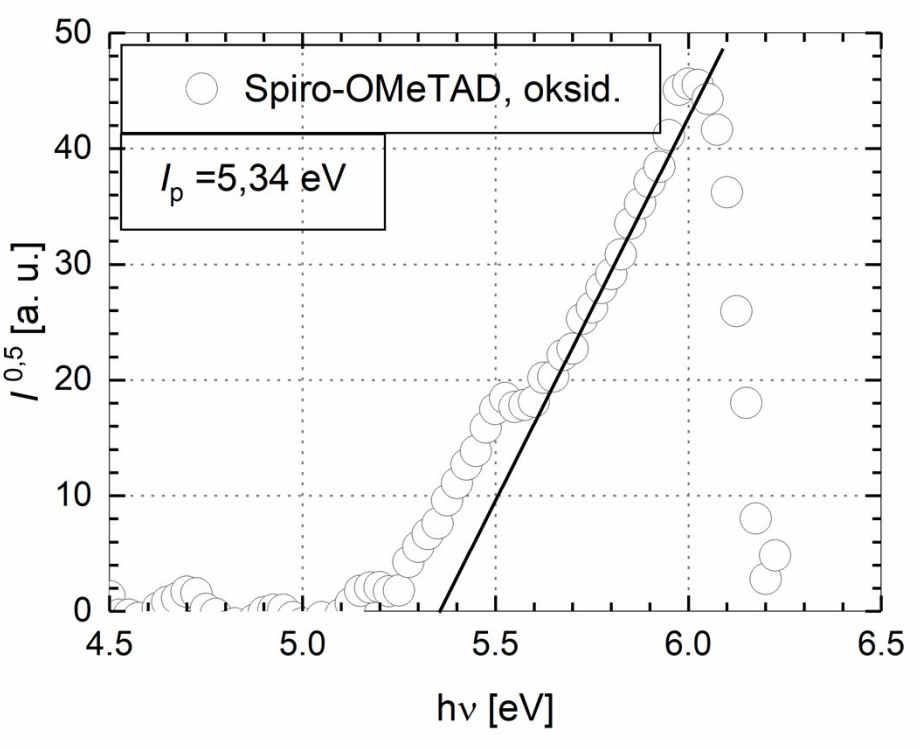


**Figure S11**. Photoemission in air spectra of the doped spiro-OMeTAD.

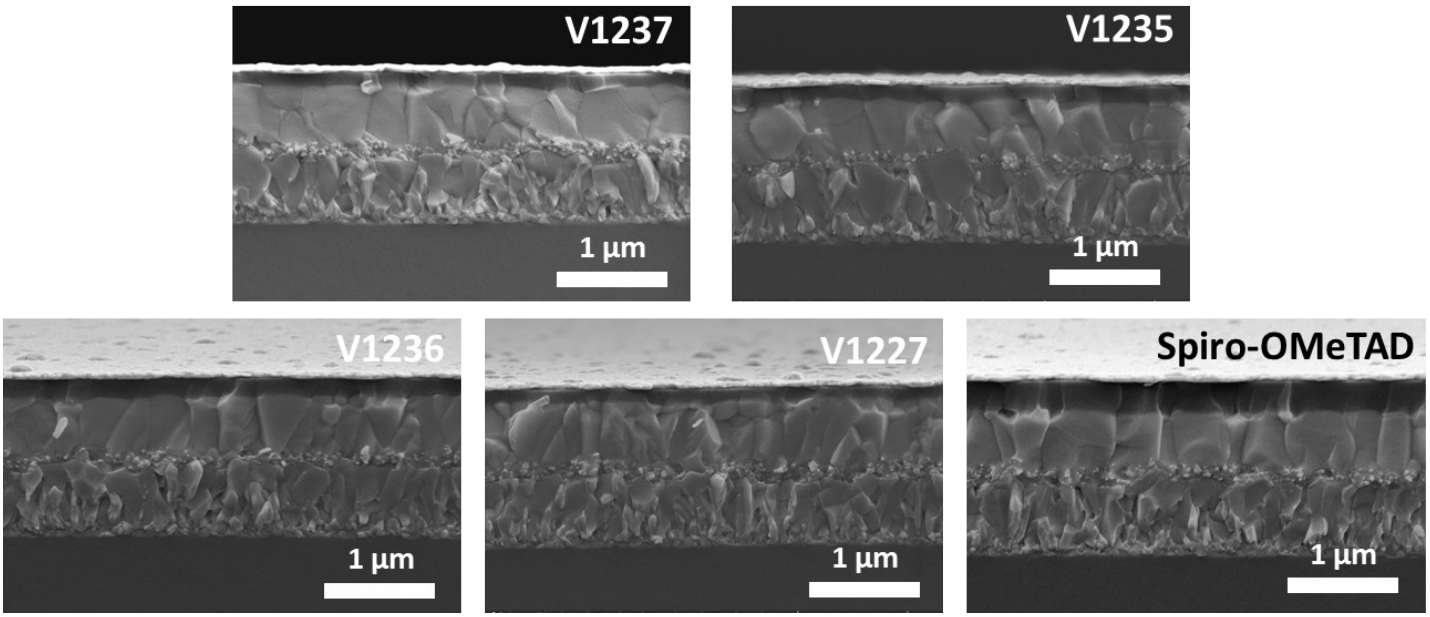


**Figure S12**. Cross-sectional SEM images of complete solar cells containing doped **V1237**, **V1235**, **V1236**, **V1227** HTMs and doped spiro-OMeTAD for comparison.

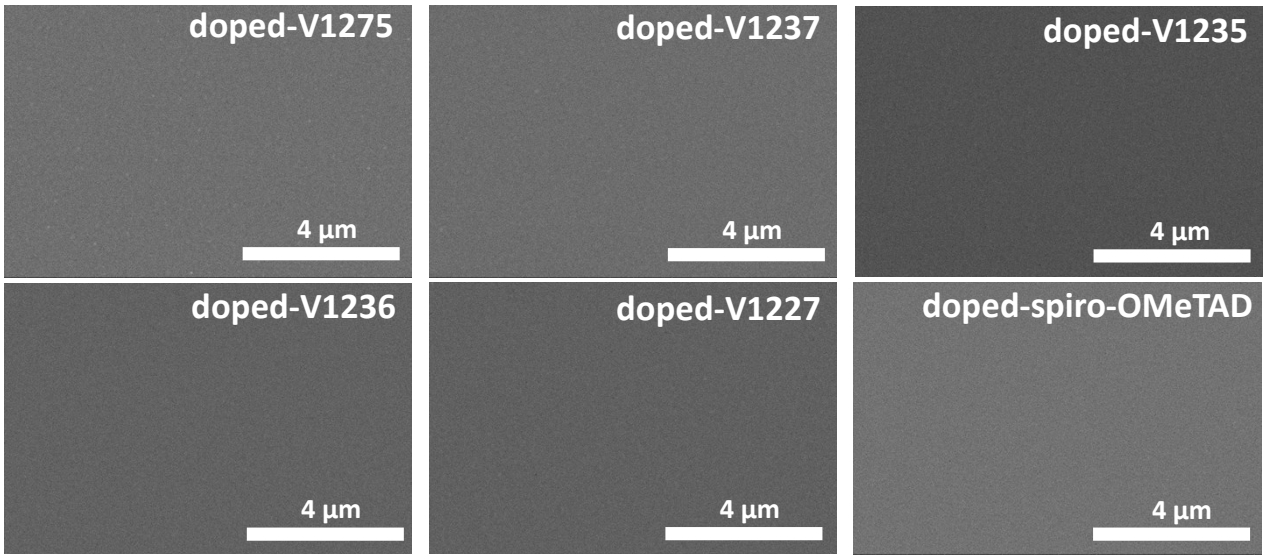


**Figure S13**. Top-view scanning electron microscope (SEM) images of doped-HTMs on FTO-glass.

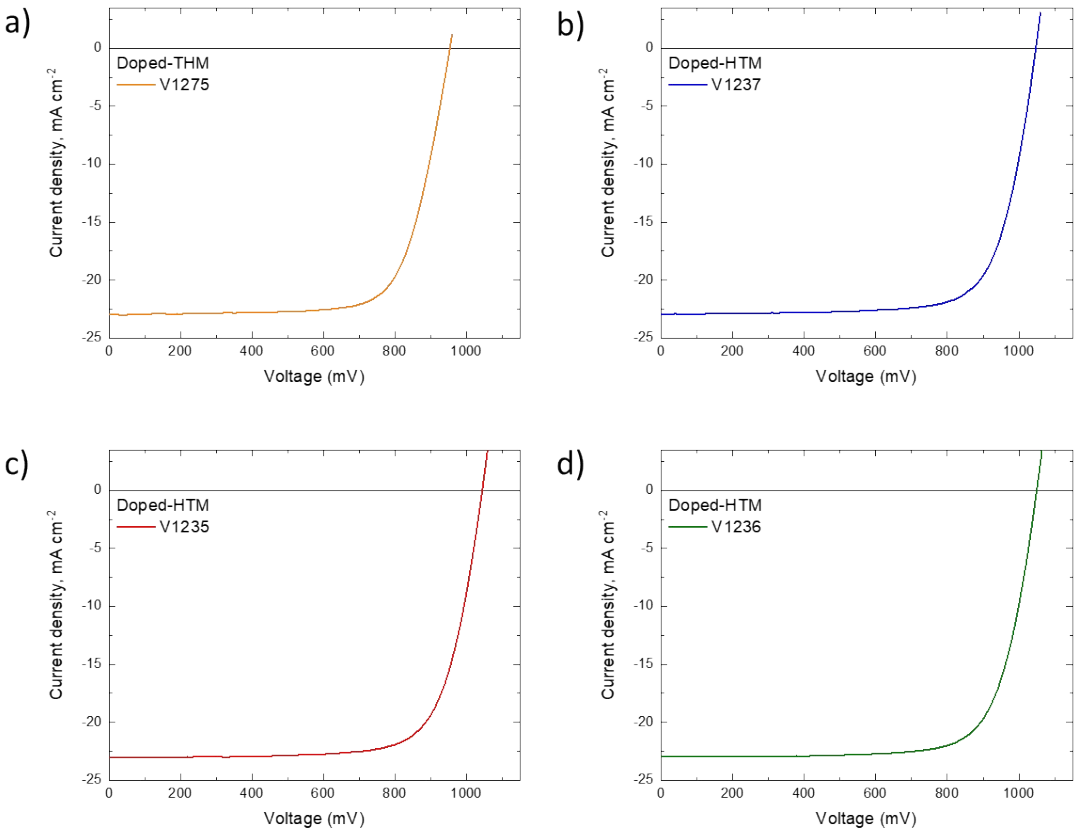


**Figure S14**. *J-V* curves of unencapsulated devices measured in a Xe-lamp solar simulator evaluated prior to the stability test.

**Table S4**. Photovoltaic parameters extracted from the initial *J-V* curves.

| | HTM | $V_{OC}$ (mV) | $J_{SC}$ (mA cm$^{-2}$) | FF | PCE (%) |
|---|---|---|---|---|---|
| **Doped-HTM** | **V1275** | 954 | 22.96 | 0.73 | 15.9 |
| | **V1237** | 1047 | 22.95 | 0.75 | 18.0 |
| | **V1235** | 1044 | 23.07 | 0.75 | 18.0 |
| | **V1236** | 1049 | 22.99 | 0.74 | 17.8 |

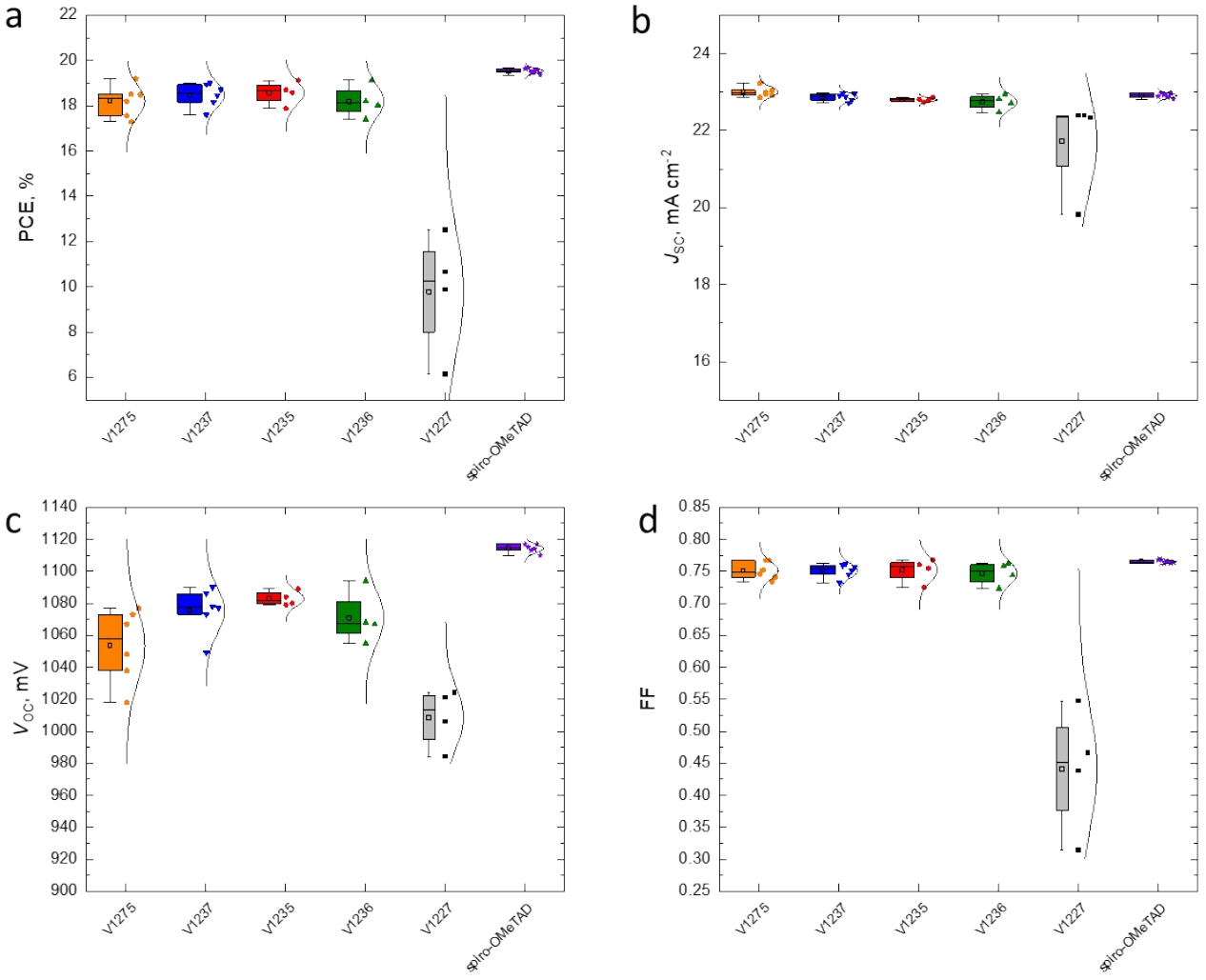


**Figure S15**. Device performance statistics of solar cells fabricated with doped **V1275**, **V1237**, **V1235**, **V1236, V1227** and -spiro-OMeTAD as HTMs. a) Power conversion efficiency, b) short-circuit current density, c) open-circuit voltage and d) fill factor. All values were extracted from the corresponding *J-V* curves.

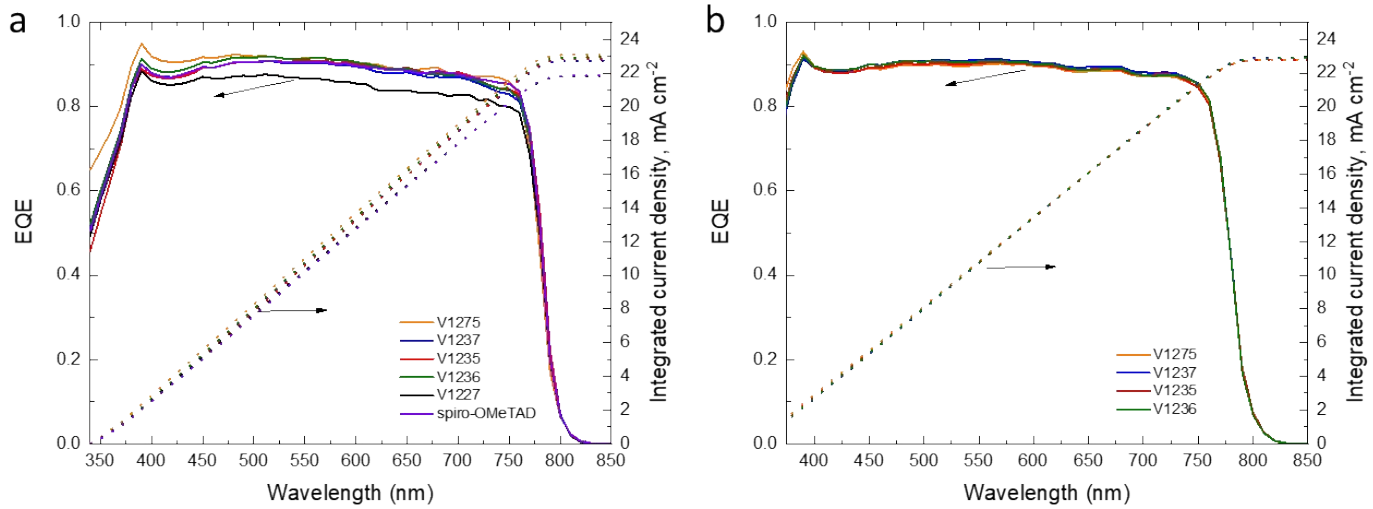


**Figure S16**. External quantum efficiency (EQE) and integrated current density of devices fabricated with a) doped HTMs and b) dopant-free HTMs.

**Table S5**. Percentage of PL quenching respect to pristine perovskite layer.

| HTM | *PL quenching (%)* |
|---|---|
| **V1275** | 52.04 |
| **V1235** | 43.48 |
| **V1236** | 68.98 |
| **V1237** | 52.60 |
| **V1227** | 54.43 |
| **spiro-OMeTAD** | 11.54 |

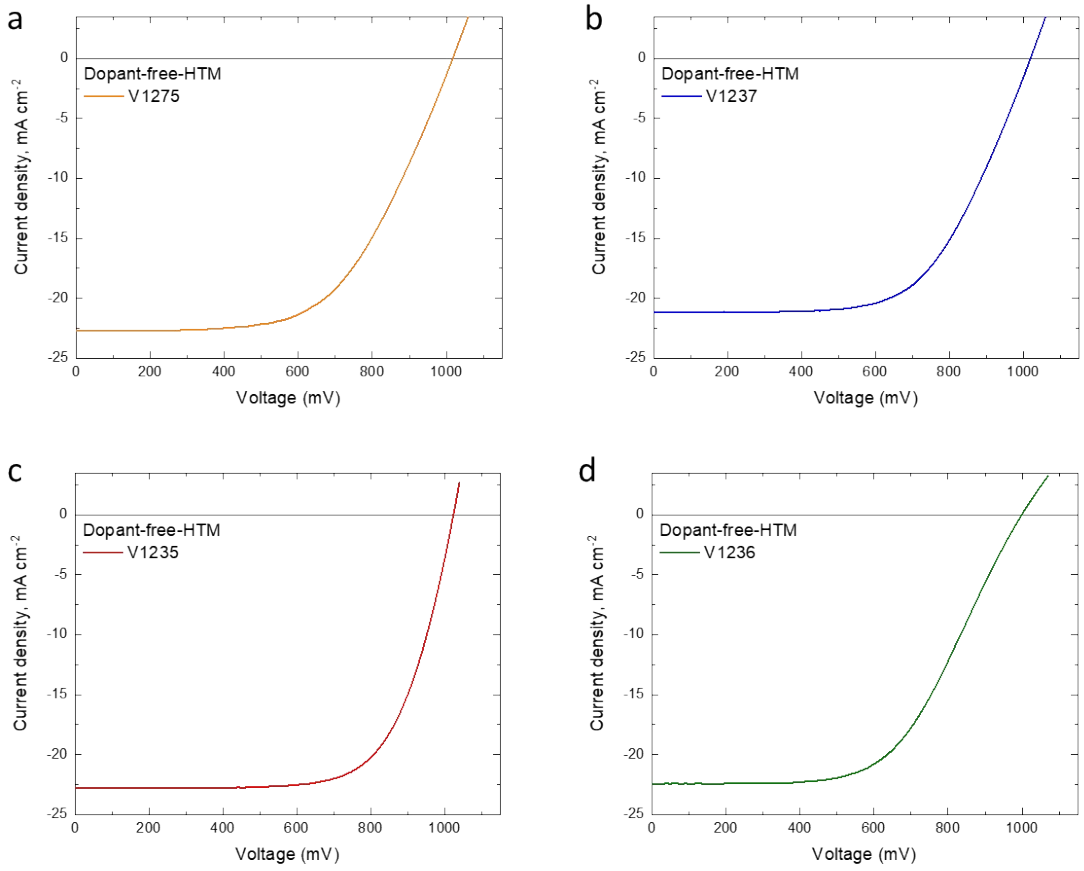


**Figure S17**. Initial *J-V* characteristics of PSCs fabricated with the dopant-free HTMs a) **V1275**; b) **V1237**; c) **V1235**; d) **V1236**.

**Table S6**. PV parameters extracted from the initial *J-V* curves of PSCs containing the dopant-free HTMs **V1275**, **V1237**, **V1235** and **V1236**.

| **HTM** | **$V_{OC}$ (mV)** | **$J_{SC}$ (mA cm$^{-2}$)** | **FF** | **PCE (%)** |
|---|---|---|---|---|
| **V1275** | 1017 | 22.71 | 0.58 | 13.4 |
| **V1237** | 1019 | 21.15 | 0.61 | 13.2 |
| **V1235** | 1024 | 22.78 | 0.69 | 16.1 |
| **V1236** | 998 | 22.44 | 0.57 | 12.8 |

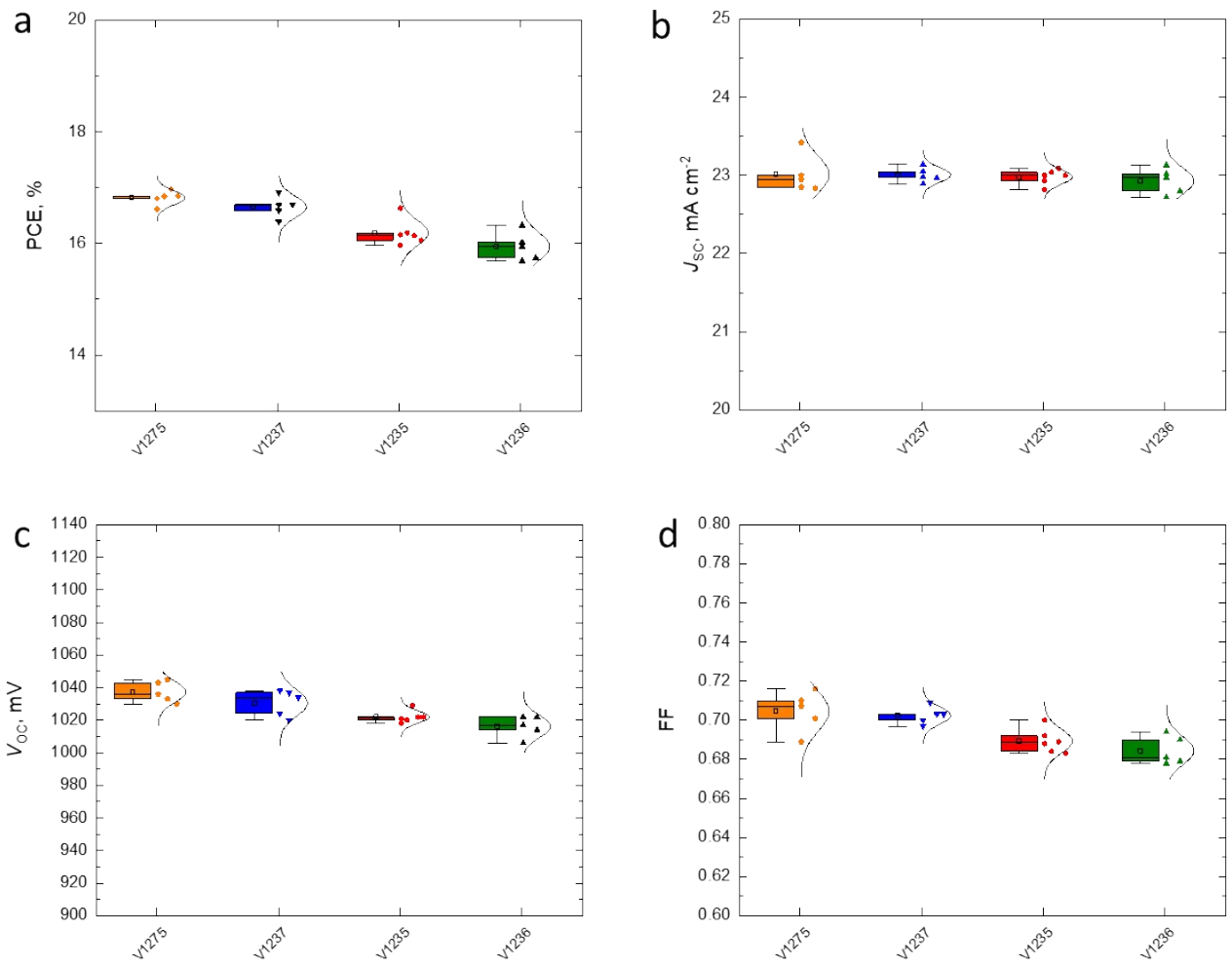


**Figure S18**. Statistics of solar cells fabricated with dopant-free **V1275**, **V1237**, **V1235**, **V1236** HTMs. a) Power conversion efficiency, b) short-circuit current density, c) open-circuit voltage and d) fill factor. All values were extracted from the corresponding *J-V* curves

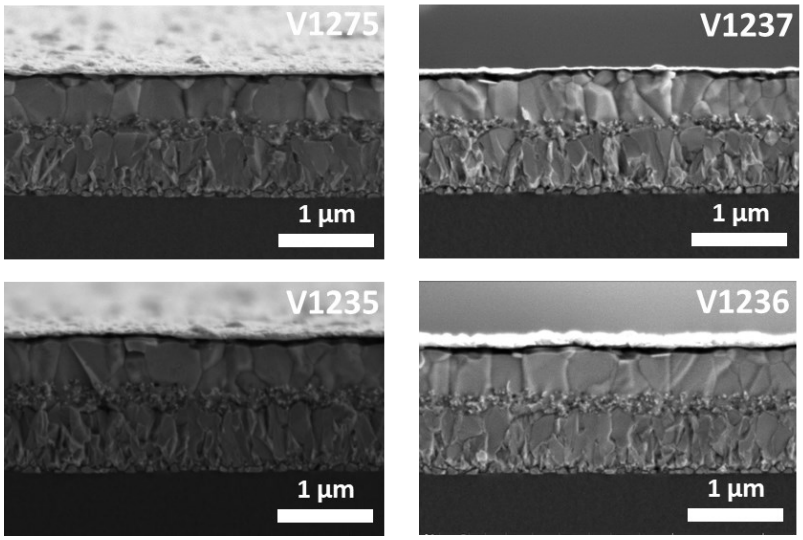


**Figure S19**. Cross-section scanning electron microscope (SEM) images of devices containing dopant-free HTMs.

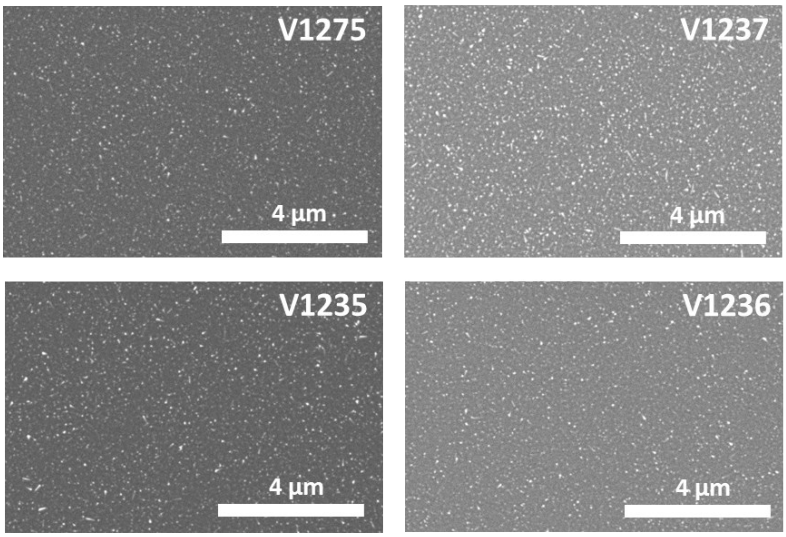


**Figure S20**. Top-view scanning electron microscope (SEM) images of dopant-free HTMs on FTO-glass.